Available online at www.sciencedirect.com

ScienceDirect

Journal of Marine Systems 68 (2007) 265 – 277

JOURNAL OF MARINE SYSTEMS

www.elsevier.com/locate/jmarsys

Inorganic carbon dynamic and air–water CO_2 exchange in the Guadalquivir Estuary (SW Iberian Peninsula)

M. de la Paz *, A. Gómez-Parra, J. Forja

Departamento de Química-Física, Facultad de Ciencias del Mar y Ambientales, Universidad de Cádiz,
Campus Río San Pedro s/n, Puerto Real (Cádiz) 11510, Spain

Received 17 April 2006; received in revised form 20 November 2006; accepted 28 November 2006
Available online 20 December 2006

Abstract

The distribution of inorganic carbon and the CO_2 exchange between atmosphere and water along the Guadalquivir Estuary (SW Iberian Peninsula) have been evaluated, on the basis of field observation performed from 2000 to 2003. The study consisted of the measurement of Total Alkalinity (TAlk), pH, continuous underway CO_2 partial pressure (pCO_2), dissolved oxygen and chlorophyll. The Guadalquivir river water is rich in TAlk and DIC and its behaviour is mainly conservative along the salinity gradient. Estuarine waters were CO_2 oversaturated in all the samplings in space and time. It has been suggested some biogeochemical processes affecting the water pCO_2 such as the CO_2 flux to the atmosphere, aerobic respiration of organic matter, and carbonate dissolution. The average CO_2 flux to the atmosphere is 85.2 mmol m^{-2} d^{-1} and the total CO_2 emission to the atmosphere is 3.2 mol C 10^6 d^{-1}. Ventilation of riverine CO_2 can contribute to the emission of CO_2 from inner estuaries although this factor seems highly variable among European estuaries. It has been estimated that, in the Guadalquivir Estuary, 34% of the total inorganic carbon exported is emitted to the atmosphere.

Keywords: Estuaries; Carbon dioxide; Dissolved inorganic carbon; Air–water fluxes; River export; Guadalquivir River

---

1. Introduction

The difference between the sources (7.1 ± 0.9 Pg C yr^{-1}, fossil fuel combustion and cement production) and sinks (5.1 ± 0.5 Pg C yr^{-1}, atmosphere and ocean) of 2 Pg C yr^{-1} for anthropogenic CO_2 is of the same order of magnitude as the overall uncertainty (±1.4 Pg C yr^{-1}) of estimation. The missing carbon sink could be the combined result of uncertainty in flux estimates and the terrestrial biosphere uptake (Sabine et al., 2004). Until recent times, the coastal ocean has been largely ignored in global budgeting efforts, even though the related flows of carbon and nutrients are disproportionately high in comparison with its surface area (Smith and Hollibaugh, 1993; Wollast, 1998). Estuaries play a significant role in the global CO_2 cycle, as they could emit around 0.43 Pg C yr^{-1}, roughly balancing the amount of CO_2 absorbed (−0.32 Pg C yr^{-1}) by all the other coastal ecosystems combined (Borges, 2005). Although high pCO_2 in all the rivers and estuaries is ubiquitous, the factors controlling pCO_2 within estuaries may vary among systems according to environmental conditions, as is the case of the Scheldt or the Amazon. Hence, simple extrapolation from these well-studied river and estuarine ecosystems to the global scale may result in inaccurate global estimates (Zhai et al., 2005). In this

---

* Corresponding author. Tel.: +34 956 01 67 41; fax: +34 956 01 60 40.
E-mail address: mercedes.delapaz@uca.es (M. de la Paz).

0924-7963/$ - see front matter © 2006 Elsevier B.V. All rights reserved.
doi:10.1016/j.jmarsys.2006.11.011

context, some investigators conclude the need for a better mapping of coastal surface CO_2, including riverine areas.

Diverse and intense mechanisms are responsible for such high levels of pCO_2 in estuaries. For instance, the residence time of the water in the estuary is the balance between the tidal effect and the river discharge, particularly in macrotidal estuaries. Increased residence time of the water in the estuary optimizes the conditions for organic matter degradation, as well as carbonate dissolution processes.

The CO_2 flux to the atmosphere is a function of the CO_2 partial pressure air–water gradient (ΔpCO_2) and the gas transfer velocity (k). Despite the availability of highly accurate and precise methods for determining ΔpCO_2, the largest source of uncertainty in the calculation of gas flux arises from the rate term k in both open ocean and coastal environment processes (Borges et al., 2004b). The ability to measure and predict atmospheric exchange accurately is limited by a lack of understanding of the mechanisms controlling k. Rivers and estuaries are systems were wind and boundary friction act as sources of turbulent energy. Laboratory experiments on transfer rates in rivers for combined wind and bottom shear-induced turbulence suggest that the processes within each regime are cumulative (Zappa et al., 2003).

Limited numbers of specific studies have been carried out on the gas transfer velocity in estuaries using methods such as dual tracer addition (Clark et al., 1995; Carini et al., 1996), natural gas tracer (Clark et al., 1992) or floating dome technique (Marino and Howarth, 1993; Borges et al., 2004a). The tracer methods involve long term measurement of the gas transfer velocity over the entire estuary, while the floating dome is a short term measurement affected by system heterogeneity typical in estuaries. The floating dome technique yields higher values compared to the other methods (Raymond and Cole, 2001) which may yield higher flux values than those actually present. In any case, the selection of a particular value for k will affect the overall representation of the net ecosystem metabolism.

In addition to the high CO_2 ventilation of riverine DIC, the fluvial export of terrestrial alkalinity is also the predominant source of oceanic alkalinity and is a key regulator of the $CaCO_3$ saturation state in the ocean, according to Raymond and Cole (2003). In this context, Huertas et al. (2006) carried out a previous study of the pCO_2 in the surface water in the north-eastern shelf of the Gulf of Cadiz, and observed a phytoplankton bloom in spring and autumn, induced by the nutrients exported from the Guadalquivir estuary. It was observed that based on annual data, the continental shelf adjacent to the Guadalquivir mouth behaves as a net sink for atmospheric CO_2.

The BIOGEST and EUROTROPH projects are among several European Union initiatives in the last decade which set out to further our understanding of trophic status in European estuaries and coastal waters, and of the mechanism involved. Until now, no study of inorganic carbon dynamics has been performed in the Guadalquivir Estuary, although the Guadalquivir is one of the largest rivers of the Iberian Peninsula as well as being the southernmost in Europe. In this study, pCO_2 and inorganic carbon distribution have been measured for the first time in the Guadalquivir estuary. Biochemical processes involved in the pCO_2 variability in time and space have been studied in relation to organic matter degradation and carbonate dissolution processes. Lastly, the air–water CO_2 fluxes and the amount of riverine carbon ventilated over the length of the estuary have been estimated.

2. Materials and methods

2.1. Study site

The 108 km long Guadalquivir estuary is located in the south-west of the Iberian Peninsula. The drainage basin of the Guadalquivir river covers an approximate area of 58,000 km^2, and the total length of the river is

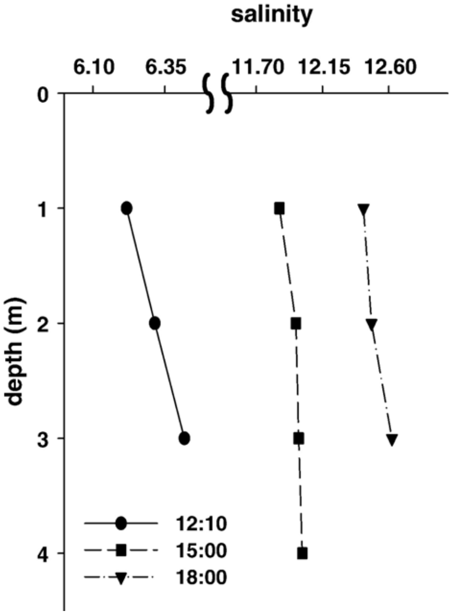

Fig. 1. Salinity profiles at different tidal stages for the anchoring sampling on June-10th 2002.

about 560 km, flowing across the south of Spain from east to west and draining into the Atlantic Ocean. The geology of the drainage basin can be divided into two parts: one of siliceous origin to the north, and a carbonate part to the south. This composition contributes to the high concentration of suspended solids and dissolved carbonates characteristic of the Guadalquivir river water.

With respect to the mixing regime and according to the classification proposed by Beer (1983), the Guadalquivir estuary is a completely mixed or vertically homogeneous estuary (see Fig. 1). Although it is surrounded by inter-tidal salt marshes, the volume of water exchange between the river and these areas is minimal in comparison to the total water volume of the estuary; owing to the regular dredging of the main channel of the river (6 m depth) to facilitate ship navigation to Seville; the estuary has an integrated cross section depth of 3 m. The Guadalquivir Estuary is characterized by an irregular river discharge, this means low discharge rates for most times of the year and extremely high rates during rainy season of February–March. The tidal velocity of around 1 m s^{-1} is 20 times the freshwater velocity, which makes the tide the main factor influencing the hydrodynamics of the estuary. The Suspended Particulate Matter (SPM) distribution along the estuary shows that the maximum turbidity zone is located around salinity 5 in the summer; nevertheless the position of this maximum is highly variable, being dependent on the tidal regime and the river discharge. The residence time of the water in the estuary, calculated from the most frequent freshwater flow (36 m^3 s^{-1}) was 18 days.

2.2. Sampling strategy

8 fixed sampling stations were selected along a 38 km stretch of the most marine part of the Guadalquivir estuary (Fig. 2, Table 1). The surveys were performed on board the R/V Mytilus in the summers of 2002 and 2003, as well as in a small vessel for the transects carried out in 2000 and 2001. In order to characterize the spatial pattern in the estuary, five transects along the salinity gradients were performed. Furthermore, to study the effects of the tidal exchange on the estuarine carbon system, continuous monitoring of the selected parameters was performed at 3 anchor stations. This tidal exchange sampling was carried out for intervals of 13 to 24 h and discrete water surface and

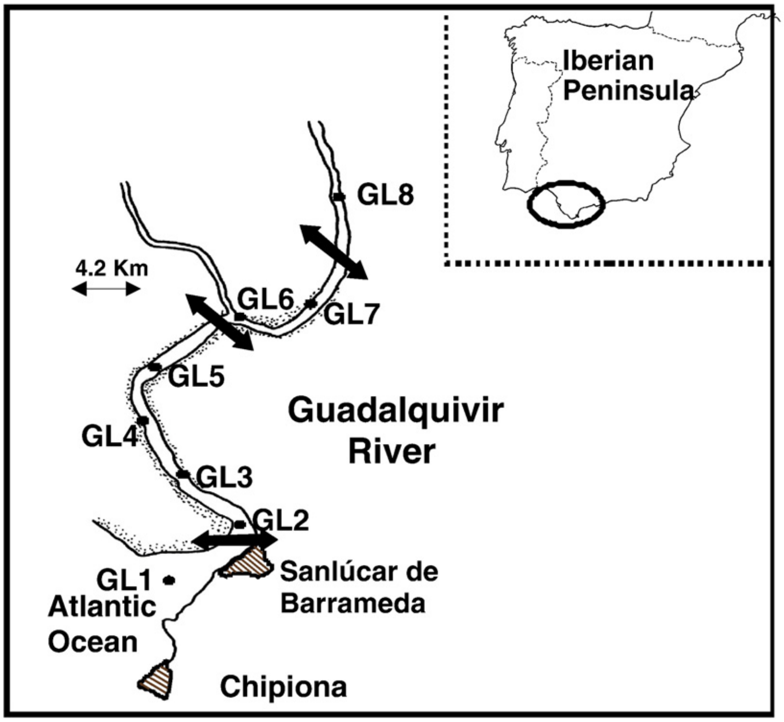

Fig. 2. Map of the Guadalquivir estuary. The 8 fixed sampling stations (●) and the locations for the tidal exchange sampling (⟷) have been indicated.

Table 1
Range for physicochemical and chemical properties of surface water for each sampling

Sampling date		Salinity	Temperature	Freshwater flow ($m^3\ s^{-1}$)	SPM ($mg\ L^{-1}$)	DIC ($mmol\ kg^{-1}$)	pH (NBS)	fCO_2 (µatm)	Total Alkalinity ($mmol\ kg^{-1}$)
19 Dec 00	Long.	2.24–32.98	15.0	13.5	33.3–171.2	2.30–4.89	7.78–8.13	518–3606	2.48–4.76
14 Nov 01	Long.	2.46–22.73	15.0	25.9	12.5–433.1	2.53–4.03	7.78–8.16	538–2640	2.70–4.01
8 Jun 02	Long.	9.79–31.67	21.0	35.1	–.	2.31–2.99	7.99–8.13	627–1027	2.51–3.09
10 Jun 02	Long.	6.81–32.11	20.9	32.1	33.3–146.0	2.26–3.09	7.97–8.17	638–1029	2.44–3.16
20 Jun 03	Long.	8.50–30.91	25.0	44.7	–	2.52–3.33	7.67–7.84	823 1617	2.58–3.34
7 Jun 02	Outer St.	19.64–36.29	21.2	43.9	65.8–543.7	2.25–2.75	7.93–8.01	581–951	2.44–2.85
8 Jun 02	Middle St.	9.74–20.52	21.3	35.1	65.8–405.8	2.66–3.04	8.00–8.18	925–1065	2.81–3.13
10 Jun 02	Inner St.	2.48–13.61	21.8	32.1	121.0–846.6	2.90–3.18	8.00–8.20	922–1165	3.00–3.20

The longitudinal samplings are indicated as *Long* while the Outer, Middle and Inner Station are reflected in Fig. 1 as the sites for tidal exchange sampling.

bottom samples were collected at 1 h intervals. Nevertheless, it would be desirable to have more information available for high rainwater runoff events (in February–March), which can considerably increase the river discharge in those months.

The underway ship's pump supplies water for the continuous measurement of salinity, temperature (Sea-Bird thermosalinometer) and CO_2 partial pressure, (sample frequency of 1 min). The oxygen was fixed in a sealed flask and stored in darkness during 24 h as described by the Winkler method, for later analysis by potentiometric titration (Metrohm 670 Titroprocessor). The samples for Dissolved Organic Carbon (DOC) were fixed with phosphoric acid and measured with a TOC-5050-A analyser (Shimatzu). Chlorophyll *a* (Chl*a*) was determined in a glass fibre filter by fluorescence after extraction in 90% acetone (Turner Designs-10 fluorometer).

The alkalinity and pH measurements of the filtered samples were carried out on the ship. The pH was measured with a glass combined electrode (Metrohm) calibrated in the NBS scale with pH 4 and 7 buffers. The alkalinity analysis was performed by the potentiometric titration methods (Metrohm 716 DMS). The alkalinity computation was made from the titration curve by means of the Gran Function and taking into account the correction for sulphate and fluoride interaction, using the constants proposed by Khoo et al. (1977) and by Perez and Fraga (1987) respectively. For the dissociation of inorganic carbon, the K1 and K2 acidity constants proposed for the NBS scale by Cai and Wang (1998), specially adapted for estuaries, as well as the K0 proposed by Weiss (1974), were selected. The method was validated with reference standards obtained from A. Dickson (Scripps Institution of Oceanography, San Diego, USA) to an accuracy of ±2 $\mu mol\ kg^{-1}$.

The equilibration technique was used to measure the continuous surface water pCO_2. The equilibration process was a mixture of laminar-flow and bubble types connected to an infrared analyser (Li-Cor 6262) according to the design of Körtzinger et al. (1996).

The wind speed data for the flux calculation were supplied from the meteorological station of the ship and daily river discharge data were provided by the Confederacion Hidrográfica del Guadalquivir (see Table 1). The water current speed was measured by means of two Aanderaa (RCM7) Current Meters, one located at the water surface and the other near the bottom.

The CO_2 gas exchange across the air–water interface can be described as a function of the gas concentration gradient and a gas exchange coefficient (k) as stated below:

$$\text{Flux } CO_2 = k([CO_2]_{\text{water}} - [CO_2]_{\text{air}})$$

where the CO_2 gradient is the driving force, and different wind speed parameterizations (which are discussed in more detail in Section 3.3) have been employed for the k calculation. The excess CO_2 is defined as the departure of free dissolved CO_2 from atmospheric concentration and is calculated as the *in situ* CO_2 concentration ($\mu mol\ L^{-1}$) minus a theoretical CO_2 concentration at equilibrium with the atmosphere at 370 µatm. The Apparent Oxygen utilization (AOU) is defined as departure of oxygen from an O_2 concentration in equilibrium with the atmosphere calculated from the Benson and Krause (1984) solubility equation.

3. Results and discussion

3.1. Longitudinal variation

In Table 1 the results for physicochemical variables obtained between 2000 and 2003 are shown. The first two transects correspond to winter and the next three to summer. The longitudinal distribution for Dissolved

Inorganic Carbon (DIC) and Total Alkalinity (TAlk) along the estuary are presented in Fig. 3. TAlk and DIC decreased as salinity increased, in relation to freshwater and seawater mixing within the estuary. The DIC and TAlk concentrations at low salinities varied within a wide range: from 3.0 mmol kg^{-1} in June 2002 to 4.9 mmol kg^{-1} in December 2000 for DIC and from 3.1 to 4.8 mmol kg^{-1} for TAlk, on the same sample dates. The higher values on TAlk and DIC in the river endmember are observed in winter. This temporal pattern was not present in the seawater endmember where less variability was found (from 2.3 to 2.5 mmol kg^{-1} in DIC).

The high TAlk concentration in the Guadalquivir river water are due to the carbonated composition of the drainage basin. The effect of this is to make the Guadalquivir River a significant source of TAlk to the adjacent zone of the Atlantic Ocean. In addition, the calcite and aragonite saturation solubility product and therefore the carbonate dissolution level increases as temperature decreases (Mucci, 1983). This explains why the higher TAlk concentration in the river endmember occurs in winter when the average temperature is 15 °C. Cai (2003) found similar values for TAlk and DIC in the near-zero salinity zone of the Mississippi River because of the high weathering rate of the drainage basin.

This is contrary to the positive slope reported in other estuaries for TAlk *vs.* salinity, indicating a higher seawater concentration than in the river (*e.g.* Devol et al., 1987; Cai and Wang, 1998; Brasse et al., 2002).

DIC is greater in the riverine part of the estuary than in the marine part; as is common in estuaries, the values being similar to those found in the Loire (Abril et al., 2003), and the Scheldt (Hellings et al., 2001), although

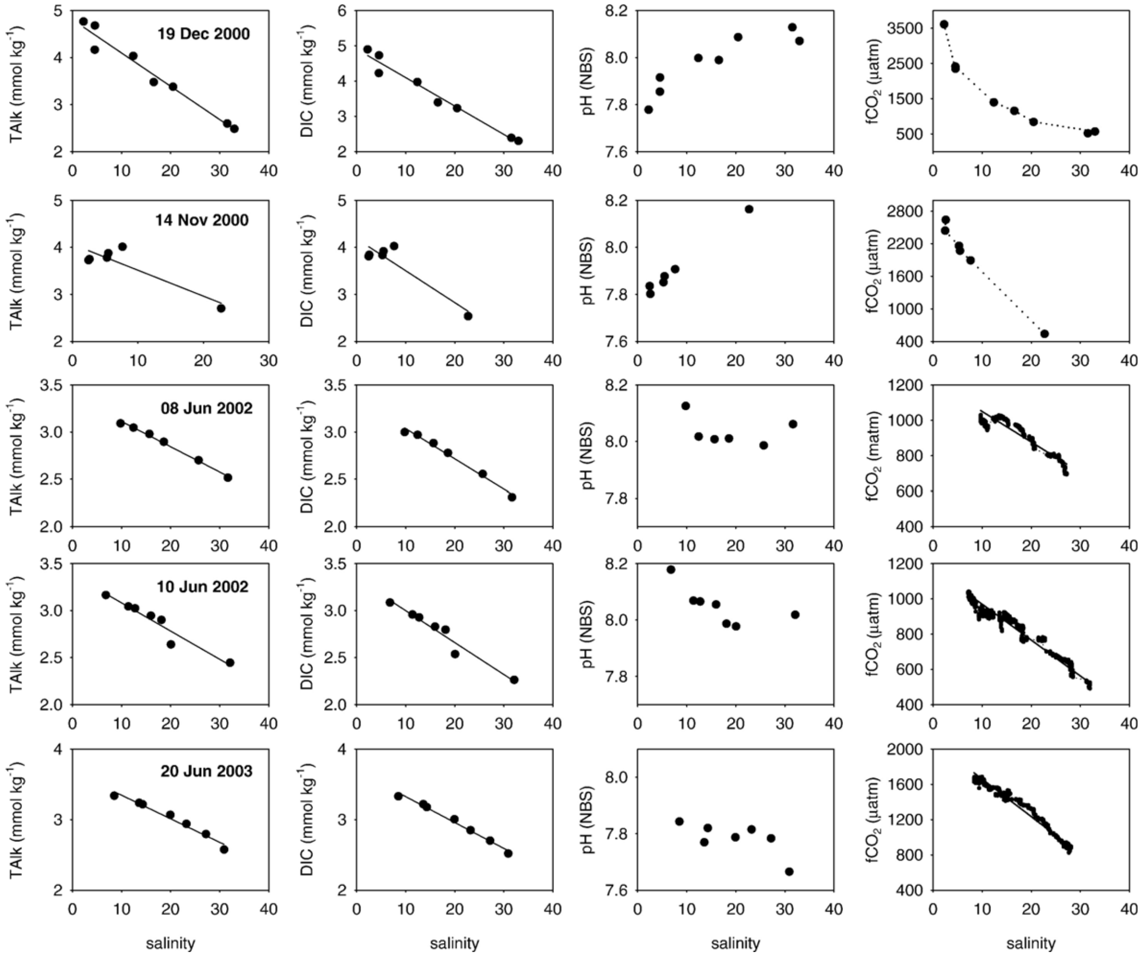

Fig. 3. Longitudinal variation of Total Alkalinity (TAlk), Dissolved Inorganic Carbon (DIC), pH and CO_2 fugacity (fCO_2) along the salinity gradient in the Guadalquivir estuary. It should be noted that no samples were gathered for stations GL7 and GL8, for transects performed on November-14th, 2000 and June-8th, 2002.

the origin of the DIC estuarine values there is different from those of the Guadalquivir River. These estuaries are characterized by high anthropogenic input of organic matter and nutrients that are responsible for intense remineralisation processes, mainly in the maximum turbidity zone.

The variation of pH (NBS) with salinity was not the same for all transects. While pH was more acid in November and December and increased with salinity (from 7.8 to 8.1/8.2), in June, upstream samples were more basic (8.0) than downstream. These seasonal variations in the pH of the river endmember are thought to be due to the change in ratios of the river source, coupled to changes in biological activity (Howland et al., 2000). During winter, the river waters are derived of the runoff, which is relatively acidic, whereas in summer, the primary production activity takes place upstream and increases the pH (accompanied by a Chl*a* maximum at low salinity, see Fig. 6).

The values of water CO_2 fugacity (fCO_2) with respect to the atmosphere were largely in excess of equilibrium values, throughout the estuary (Table 1, Fig. 3). In the case of fCO_2, a linear relationship *vs.* salinity was found in most of the longitudinal samplings. The river water presented elevated fCO_2 values, related to the high levels of DIC found in the Guadalquivir River. The maximum value for fCO_2 of 3605 µatm was observed upstream in December 2000 with the minimum being recorded in June 2002 with a value of 1029 µatm. For the summer samplings, the slight differences amongst the 2002 transects are due to variations in the river discharge and tidal coefficient. The Guadalquivir estuary follows common trends and presents a similar range of fCO_2 values when compared to other European estuaries, such as the Elbe (Brasse et al., 2002), Rhine and Gironde (Frankignoulle et al., 1998) and Loire (Abril et al., 2003).

Assuming salinity is a satisfactory mixing indicator, then for any dissolved constituent subject only to physical mixing processes, the resultant plot will be linear, with a negative slope for components which are more concentrated in freshwater than in seawater (Liss, 1976). Table 2 represents the linear regression equation for DIC *vs.* salinity, where C_0 is the DIC concentration in freshwater, calculated from the equation at zero salinity. It can be deduced that the behaviour of DIC is conservative and that the main source of DIC to the estuary is from the freshwater; hence there is no apparent net reaction. The DIC export from the river to the adjacent coastal areas is the product of the freshwater discharge and the freshwater DIC concentration. The DIC export obtained varied from 5.7×10^6 mol d^{-1} in December 2000 to $14{,}2\times10^6$ mol d^{-1} in June 2003. In the Guadalquivir estuary, the high DIC export is due mainly to the high TAlk concentration in the river and not to internal addition as in the case of the Scheldt (Hellings et al., 2001) or the Loire (Abril et al., 2003) estuaries.

3.2. Tidal variations

Semi-tidal cycles were performed at three different sites in the estuary in order to study the tidal influence on the inorganic carbon system. These sites were located to cover the maximum salinity range associated with tidal variation. The Outer Estuary Station was the most marine site (near GL2, see Fig. 2) with the salinity ranging from 19.6 to 36.3 (Table 1); salinity at the Middle Estuary Station (near GL6) varied between 9.7 and 20.5; and at the more fluvial anchoring station referred to as the Inner Estuary Station (between GL7 and GL8) salinity ranged from 2.5 to 13.6.

In this context previous research has been done to study the tidal effect on the inorganic carbon cycle in estuaries (Raymond et al., 1997), marshes (Neubauer and Anderson, 2003) or mangroves (Biswas et al., 2004), as well as in laboratory simulations (García-Luque et al., 2005).

Fig. 4 shows tidal cycle effects and illustrates the marine and freshwater mixing within the estuary. The friction phenomenon along the estuary combined with the river discharge means that the tidal wave does not behave symmetrically. As a result, there is a slight disphase between the salinity maximum and the high tide.

Table 2
Parameters of the linear fittings of DIC *vs.* salinity; the river DIC concentration (C_0), freshwater flow (Q) and the calculated DIC export defined as ($C_0 \cdot Q$) have been included

Date	Slope (mmol kg^{-1} psu^{-1})	C_0 (mmol kg^{-1})	r^2	Freshwater flow (m^3 s^{-1})	Export of DIC 10^6 (mol d^{-1})
19 Dec 00	−0.081	4.91	0.97	13.51	5.72
14 Nov 01	−0.068	4.18	0.86	25.86	9.33
08 Jun 02	−0.032	3.36	0.99	35.12	10.17
10 Jun 02	−0.034	3.34	0.95	32.14	9.26
20 Jun 03	−0.037	3.70	0.99	44.69	14.23

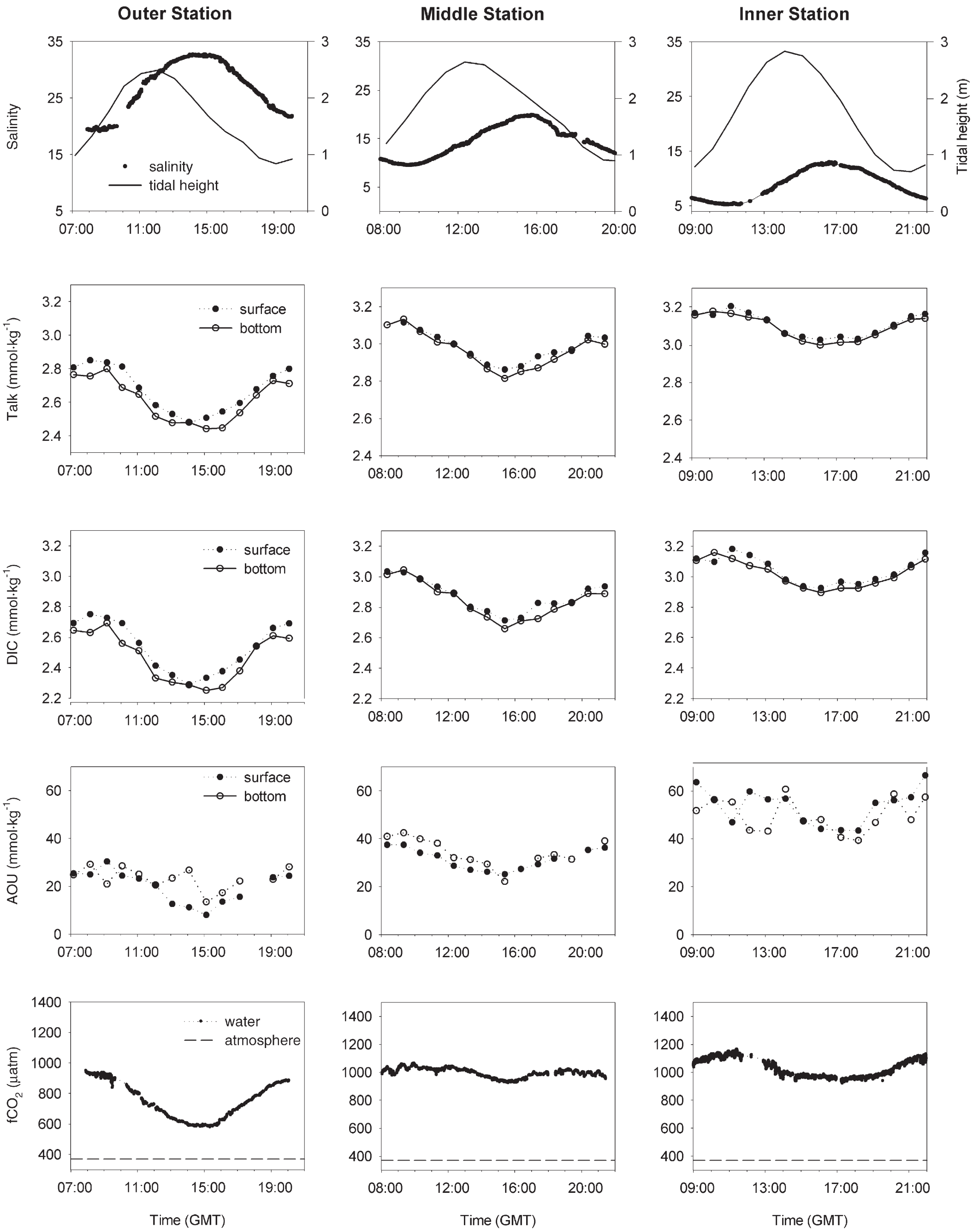

Fig. 4. Tidal variation of tidal height, salinity, Total Alkalinity (TAlk), Dissolved Inorganic Carbon (DIC), Apparent Oxygen utilization (AOU) and CO_2 fugacity (fCO_2).

As is the case for the salinity gradient distribution, maximum salinities are linked to minimum TAlk, DIC, AOU and fCO_2. There were no significant differences found between the surface and bottom concentrations, which corroborates the theory that the Guadalquivir is vertically homogeneous (or a completely mixed estuary). Minimum values of TAlk were found in the Outer Station (2.47 to 2.85 mmol kg^{-1}) and higher values were found upstream due to the increase in the influence of fluvial water, while the tidal variability decreased. Variations for TAlk were 0.38 mmol kg^{-1} at the Outer Station, 0.26 mmol kg^{-1} at the Middle and 0.18 mmol

kg^{-1} TAlk at the Inner Station. For DIC the variations were 0.46 mmol kg^{-1} at the Outer Station, 0.32 mmol kg^{-1} at the Middle Station and 0.26 mmol kg^{-1} at the Middle Station.

The $f\mathrm{CO_2}$ of the surface water at the Outer Station presented a minimum at high tide of 580 µatm, and reached 950 µatm at low tide. At the Middle Station, high tide to low tide values varied from 925 to 1065 µatm, and Inner Station values ranged from 922 to 1165 µatm. Anchor monitoring revealed that tidal variability is noticeably higher in the most marine station when compared with the more fluvial estuary, and water advection is the key factor controlling the TAlk, DIC and AOU (Apparent Oxygen utilization) variability.

Diurnal changes accounted for an insignificant amount of the total change as indicated by the minimal difference in $f\mathrm{CO_2}$, DIC and TAlk values between similar tidal phases. It can be deduced that the river discharge is more efficient than the tidal effect in the net transport of TAlk and DIC to offshore waters, and that the main factor, especially for macro-tidal estuaries, is the residence time of both water and suspended matter in the estuary (Wang and Cai, 2004).

Different biogeochemical processes may be associated with the surface water $p\mathrm{CO_2}$ in the Guadalquivir estuary. The main processes involved are inorganic carbon respiration, carbonate dissolution and gas exchange with the atmosphere. Apart from in highly reduced waters, it can be considered that oxygen depletion is close to the fraction of excess CO_2 produced by heterotrophic processes (Abril et al., 2000). Previous work in estuaries has applied the relationship between excess CO_2 and AOU in a quantitative approach of the stoicheiometry of the organic matter respiration processes (Ballester et al., 1999; Zhai et al., 2005).

The excess CO_2 *vs.* AOU relationship was plotted (Fig. 5) for the combined set of surface anchoring data. Excess CO_2 was calculated using the measurement taken from the equilibrator.

It can be observed that there is an increase in excess CO_2 with the AOU. Excess CO_2 varied from 6.85 to 27.81 µmol kg^{-1} while AOU values ranged between 8.01 and 66.49 µmol kg^{-1}, the higher values corresponding to the upper estuary. The values found in the Guadalquivir estuary for excess CO_2 and AOU are relatively low compared to the amounts found in other estuaries, like the Piracacaba River, Brasil (Ballester et al., 1999) or the Perl River, China (Zhai et al., 2005), characterized by high organic matter inputs.

The slope of the plot for excess CO_2 *vs.* AOU at the Outer Station is 0.62. Analogous values are found in Zhai et al. (2005), which also contains references to the elemental composition of the organic matter in estuaries. However, the slopes for the Inner and Middle Stations decrease to 0.28 and 0.24 respectively, suggesting the occurrence of other non-metabolic processes that remove CO_2 from the water column in this zone of the estuary.

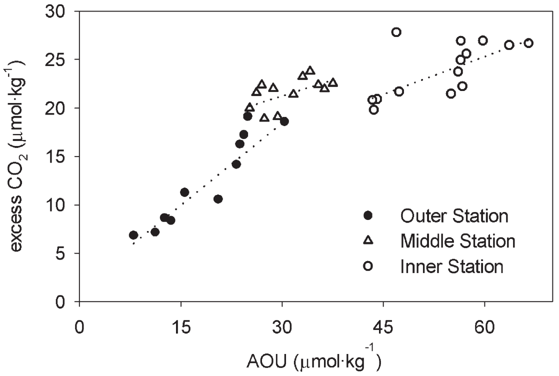

Fig. 5. Excess CO2 *vs.* Apparent Oxygen utilization (AOU). The equations for the regression lines are: Inner station ($y=0.24x+10.925$, $r^2=0.5$), Middle station ($y=0.28x+12.86$, $r^2=0.65$), Outer station ($y=0.62x+0.81$, $r^2=0.89$).

Due to the high levels of HCO_3^- present in the estuary, it is possible to estimate the excess CO_2 in the free gas form (Ballester et al., 1999; Zhai et al., 2005) rather than the DIC form (DeGrandpre et al., 1997; Abril et al., 2003), under the assumption that the contribution of CO_2 dissolved from the organic matter respiration is negligible when the predominant effect of the bicarbonate buffer HCO_3^- is taken into account.

The entire set of data points of the 3 anchoring samplings are displayed together *vs.* salinity in order to portray the space–time variability in the concentration of Chl*a*, DOC and Suspended Particulate Matter (SPM) (Fig. 6).The Dissolved Organic Carbon (DOC) concentration *vs.* salinity curve (Fig. 6) shows an increase in DOC towards the fluvial section, and a much more scattered pattern within the maximum turbidity zone. This may be due to internal or lateral contributions from the adjacent rice fields and salt marshes, since the average Chlorophyll *a* concentration in the Guadalquivir of 6.7 µg L^{-1} is not sufficient to sustain such levels of DOC through exudation. Abril et al. (2002) develop a cross comparison of organic carbon origin in estuaries, arguing that two major variables control the intensity of the organic carbon mineralisation: the lability/origin of the organic carbon, and the residence time of the particle in the estuary. The case of the Guadalquivir is comparable to that of the Sado and Ems estuaries whose DOC concentrations range from 1.9 to 9.6 mg·L^{-1} (Abril et al., 2002). The distribution of DOC may support in part the increase in the respiration processes

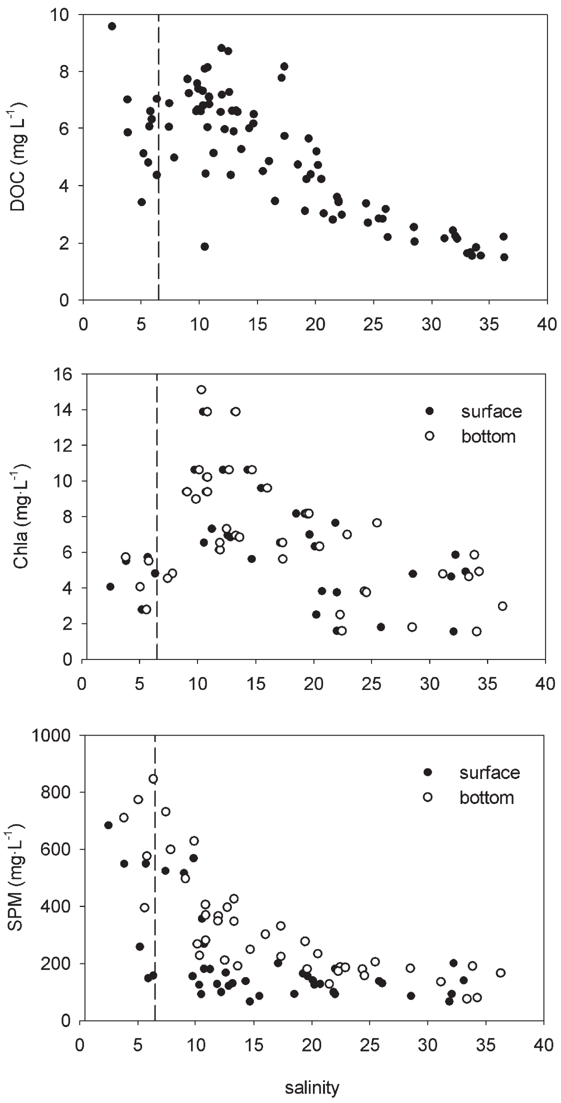

Fig. 6. Dissolved Organic Carbon (DOC), Chlorophyll (Chl*a*) and Suspended Particulate Matter (SPM) *vs.* salinity for the three tidal exchange sampling data in 2002. Vertical dashed line shows the location of the maximum turbidity zone.

toward the upper estuary, although it is not an intense process in the estuary.

Another possible mechanism responsible for buffering the increased $p\mathrm{CO}_2$ values caused by the remineralisation of organic carbon is carbonate mineral dissolution, which can be represented by the following equation:

$$\mathrm{CO_2 + H_2O + CaCO_3 = Ca^{2+} + 2HCO_3^-}$$

The calcite and aragonite solubility product (K_{sp}) (Mucci, 1983) for the Guadalquivir can be calculated as a function of the salinity and temperature as well as the saturation index. Despite the water column being oversaturated in calcite and aragonite, $\mathrm{CaCO_3}$ dissolution is able to take place. This dissolution is more significant at the bottom and in the maximum turbidity zone (dissolved suspended matter >400 mg $\mathrm{L^{-1}}$), where the resuspension of the particulate material provides sufficient time and so increases the probability of reaction. Jahnke and Jahnke (2000) observed that, although the bottom water was significantly supersaturated with respect to calcite and aragonite, $\mathrm{CaCO_3}$ dissolution was found to occur in the pore water of the superficial sediment, as a result of acidification related to organic matter oxidation.

It was hypothesized that the mechanism involved in the departure from the expected $\mathrm{CO_2}$ concentration in the water was due to carbonate dissolution. Additional information regarding the $\mathrm{Ca^{2+}}$ distribution along the estuary as well as sediment DIC and TAlk fluxes would assist in properly accounting for these processes. Detailed studies of this carbonate dissolution mechanism in the Loire (Abril et al., 2003), Gironde (Abril et al., 1999) and Seine (Roy et al., 1999) estuaries, have each taken into account the dissolution/precipitation processes in carrying out a carbon balance over the entire estuary.

3.3. Estuary-atmosphere $\mathrm{CO_2}$ exchange

Fluxes for the Guadalquivir Estuary are calculated using various estuarine gas transfer parameterizations: a) O'Connor and Dobbins (1958) proposed an oxygen re-aeration rate as a function of the water current velocity and water column depth; b) Borges et al. (2004b) constructed an empirical relationship based on floating dome measurement in the Scheldt estuary that accounted for the wind stress effect and the current speed, using the relationship from O'Connor and Dobbins (1958); c) Carini et al. (1996) studied the gas transfer velocity in Parker River Estuary using $\mathrm{SF_6}$ addition; and d) Clark et al. (1995) derived an expression based on $\mathrm{SF_6}$ tracer measurement in the Hudson River and $^{222}\mathrm{R}$ mass balance in San Francisco Bay. After estimating the k using different algorithms, it has been converted to *in situ* temperature and density assuming a dependency of k proportional to $\mathrm{Sc}^{-0.5}$. Sc was computed for *in situ* conditions using the Wanninkhof (1992) relationship and assuming that Sc varies linearly with salinity.

The estuary has been divided into three sections for the $\mathrm{CO_2}$ flux calculation using the data from the anchoring sampling. The result for the $\mathrm{CO_2}$ gas transfer velocities within the estuary, as well as the wind speed and tidal current, are shown in Table 3. The daily wind velocity was highly random and variable oscillating between 5.0 m s^{-1} and 9.8 m s^{-1}. The maximum tidal current (from 60 cm s^{-1} to 99 cm s^{-1}) is explained by bathymetry and seawater/freshwater mixing values. The use of different parameterization can provide information on the spatial variability of k along the estuary because the relationship is strongly affected by the processes dominant at each station. The parameterization proposed by Borges et al. (2004b) gave the highest values throughout the estuary, followed by k_{Clark} for high wind speed and by k_{Carini} for lower wind speed. This is because the k_{Clark} relationship with wind speed is quadratic while for k_{Carini} the relationship is linear. The maximum k values correspond to the Middle Station, where the wind speed computed that day was especially high. The expression of O'Connor and Dobbins (1958) produced the minimum k values since it considers water current alone. The values for $k_{\mathrm{O'Connor}}$ are in the same range as those found by Zappa et al. (2003), who described a daily variability in k from 2.2 to 12 cm h^{-1} for a low wind day in the Hudson estuary. The water current effect is estimated by applying the ratio as the ratio $k_{\mathrm{O'Connor}}/k_{\mathrm{O'Connor}}+k_{\mathrm{Carini,}}$, representing around 30% of the gas transfer velocity along the estuary which is rather high yet comparable to other European macro-tidal estuaries such as the Scheldt (Borges et al., 2004b). The maximum contribution of the water current corresponds to the Inner Station owing to the reduced cross-section which creates higher friction, but in no case is it comparable to the wind speed effect.

Following the consideration of Borges et al. (2004b) that the water current and wind speed have an additive effect on the gas transfer velocity, it was decided to select a combination of a) the wind speed parameterization proposed by Carini et al. (1996) based on tracer addition technique which gives a best estimate for long term spatial and temporal scales, and also because of the morphological similarities between the Park River and Guadalquivir River estuaries; and b) the water current expression from O'Connor and Dobbins (1958). The additive result will be $k = k_{\mathrm{O'Connor}} + k_{\mathrm{Carini}}$.

Table 3
Daily average wind speed, maximum tidal current speed, air–water CO_2 concentration gradient and different parameterization for CO_2 gas transfer velocity in the three sections of the Guadalquivir estuary

	Outer Station	Middle Station	Inner Station
Wind speed (m s^{-1})	7.9±2.0	9.8±3.2	5.0±1.9
Maximum tidal current speed (cm s^{-1})	84±9	60±6	99±14
ΔpCO_2 (µatm)	362.3±116.2	601.1±32.2	673±59
k_{Borges} (cm h^{-1})	27.2±4.8	32.6±8	22.1±3.5
k_{Clark} (cm h^{-1})	17.6±7.6	27.6±13.6	8.6±3.5
k_{Carinni} (cm h^{-1})	15.8±3.9	17.3±6.5	10.4±2.8
$k_{\mathrm{O'Connor}}$ (cm h^{-1})	7.1±1.9	6.1±1.9	8.0±2.4
Water current contribution %	30±8	28±15	41±12

Gas transfer velocity relationship: k_{Borges} (wind+water current), k_{Clark} (wind), k_{Carini} (wind) and $k_{\mathrm{O'Connor}}$ (water current). The water current contribution (%) was calculated as the ratio $k_{\mathrm{O'Connor}}/k_{\mathrm{O'Connor}}+k_{\mathrm{Carini}}$.

Table 4
Area, average air–water pCO_2 gradient, air–water CO_2 flux and CO_2 emission at each estuarine station in summer time

	Outer Station	Middle Station	Inner Station
Area (km^2)	26.24	7.39	4.95
ΔpCO_2 (µatm)	362.3±116.2	601.1±32.2	673.0±59
Air–water CO_2 Flux (mmol m^2 d^{-1})	68.9	114.3	128
CO_2 emission (10^6 mol C d^{-1})	18.1	8.45	6.33

An average gas transfer velocity for the entire estuary of $k=22.5$ cm h^{-1} has been used.

An average gas transfer velocity has been calculated to avoid the high spatial and temporal heterogeneities associated with wind speed measurement and tidal current velocity. The average wind speed for the sampling period was 7.35 m s^{-1} with an average tidal velocity reported of 0.54 m s^{-1}, and an integrative depth value for all the estuary of 3 m. The resultant gas exchange velocity (k) for the Guadalquivir Estuary is 22.5 cm h^{-1}.

CO_2 flux to the atmosphere in the distinct sections of the Guadalquivir estuary evaluated using k were: 68.9 mmol m^{-2} d^{-1} at the Outer Station, 114.3 mmol m^{-2} d^{-1} at the Middle Station and 128 mmol m^{-2} d^{-1} at the Inner Station. The air–water CO_2 flux data has been summarized in Table 4. The daily flux to the atmosphere can be calculated by multiplying the CO_2 flux value by the area in question, with the result that CO_2 emissions at the Outer Station were 1.8 10^6 mol C d^{-1}, 0.85 10^6 mol C d^{-1} at the Middle Station and 0.63 10^6 mol C d^{-1} at the Inner Station. It should be pointed out that the estuary has been divided according to the salinity range and not the area-width distribution. This may explain the apparently disproportionate range of emission values in the different stations. To calculate the average daily flux over the entire estuary, CO_2 emission for the entire estuary (the sum of the emissions calculated for each area) was divided by the total estimated area of the Guadalquivir estuary. The average daily flux in the Guadalquivir is 85.2 mmol m^{-2} d^{-1} and the total CO_2 emission is 3.2 10^6 mol C d^{-1}.

Opposite distribution between flux and emission is the common pattern found in estuaries. Several recent compilations are found about CO_2 emission in European inner estuaries (Frankignoulle et al., 1998; Abril and Borges, 2004; Borges, 2005) but no data up to this time has been available for the Guadalquivir Estuary. The average daily flux in the Guadalquivir estuary is analogous to the data found in Borges (2005) for the Sado (Portugal), Gironde (France) and Rhine (Netherland). Huertas et al. (2006) estimated that CO_2 fluxes in the continental shelf adjacent to the Guadalquivir estuary oscillated between a CO_2 source of 0.8 mmol m^2 d^{-1} in summer and a net uptake in October of 2 mmol m^2 d^{-1}. It is worth noting the intensity of the fluxes in the inner estuary compared to the continental shelf.

3.4. Carbon balance in the Guadalquivir Estuary

This study deals with the summer inorganic carbon balance which includes the fluvial DIC input, the DIC output to the Atlantic Ocean and the air–water flux of CO_2. In this case, the conservative DIC distribution along the estuary implies that river input and DIC export balance out. This does not mean that no processes affect the DIC as it passes along the estuary; rather that the CO_2 flux to the atmosphere must be balanced by net CO_2 production processes in the water column or sediment. These processes are organic matter degradation and calcium carbonate dissolution, the former producing CO_2 and the latter consuming CO_2. Nevertheless, for the average CO_2 flux to the atmosphere and average DIC concentration (85 mmol m^{-2} d^{-1} and 3 mmol kg^{-1} respectively) the one day emission to the atmosphere represents 0.9% of the total water column DIC budget. This is not significant compared to the high longitudinal DIC gradient in the Guadalquivir estuary.

DIC exported includes flux to the atmosphere, which reaches 3.2 10^6 mol C d^{-1}, compared with export to the Atlantic Ocean of 9.7 10^6 mol C d^{-1}. It can be concluded that 25% of the DIC exported from the Guadalquivir Estuary is emitted to the atmosphere, and 30% of the riverine DIC is ventilated. The percentage of riverine DIC ventilated to the atmosphere is highly variable from one estuary to another. Among European estuaries, the Douro and the Randers Fjord currently represent the highest and lowest reported levels of air–sea flux, respectively (Borges et al., 2006). Abril et al. (2000) estimated that in the Scheldt the riverine origin of CO_2 emission is about 10% while in the Randers Fjord the river contribution reaches 50%.

4. Conclusions

The results presented in this study provide a description of the inorganic carbon distribution along the Guadalquivir estuary. The fluvial water is rich in TAlk and the estuary acts as a net exporter of TAlk and DIC to the adjacent coastal water. The TAlk river concentration presents a seasonal variability with higher concentrations in winter than in summer. The average DIC export from the Guadalquivir is 9.7 10^6 mol C d^{-1}. Although the behaviour of the TAlk and inorganic carbon is mainly conservative along the estuary, some biogeochemical processes can co-occur, such as the aerobic respiration processes in organic matter which produce CO_2 in the water column, and the carbonate dissolution process that causes a slight decrease in CO_2 concentration in the water, even when it is originated by the superficial sediment. Moreover, CO_2 efflux has been estimated from the CO_2 air–water gradients and gas transfer coefficients that take into account the tidal current and the wind speed effects. Comparison of the different parameterization available was carried out.

Neither the organic matter respiration nor the carbonate dissolution reaction play the major role, as is the case for many European estuaries, where internal DIC production is significant, such as in the Scheldt and Loire. In this case study, these aforementioned processes have been proposed to balance the CO_2 flux to the atmosphere.

The average CO_2 flux to the atmosphere was 85 mmol m^{-2} d^{-1} while the total CO_2 emission to the atmosphere was 3.2 10^6 mol C d^{-1}. Ventilation of riverine CO_2 can contribute to the emission of CO_2 from inner estuaries although it seems highly variable. In the Guadalquivir 25% of the carbon exported is emitted to the atmosphere.

Acknowledgments

This work was supported by the Spanish CICYT (Comisión Interministerial de Ciencias y Tecnología) of the Ministerio de Educación y Ciencia under contract CTM2005 01364/MAR. Thanks to the crew of the R.V. Mytillus for the collaboration during sampling tasks.

References

Abril, G., Borges, A.V., 2004. Carbon dioxide and methane emissions from estuaries. In: Trembaly, A., Varfalvy, L., Roehm, C., Garneau, M. (Eds.), Greenhouse Gases Emissions from Natural Environments and Hydroelectric Reservoirs: Fluxes and Processes. Springer, Berlin, pp. 187–212.

Abril, G., Etcheber, H., Le Hir, P., Bassoullet, P., Boutier, B., Frankignoulle, M., 1999. Oxic/anoxic oscillations and organic carbon mineralization in an estuarine maximum turbidity zone (The Gironde, France). Limnol. Oceanogr. 44, 1304–1315.

Abril, G., Etcheber, H., Borges, A.V., Frankignoulle, M., 2000. Excess atmospheric carbon dioxide transported by rivers into the Scheldt estuary. Earth Planet. Sci. Lett. 330, 761–768.

Abril, G., Nogheira, E., Etcheber, H., Cabecadas, G., Lemaire, E., Brogueira, M.J., 2002. Behaviour of organic carbon in nine contrasting European estuaries. Estuar. Coast. Shelf Sci. 54, 241–262.

Abril, G., Etcheber, H., Delille, B., Frankignoulle, M., Borges, A.V., 2003. Carbonate dissolution in the turbid and eutrophic Loire estuary. Mar. Ecol., Prog. Ser. 259, 129–138.

Ballester, M.V., Martinelli, L.A., Krusche, A.V., Victoria, R.L., Bernardes, M., Carmago, P.B., 1999. Effects of increasing organic matter loading on the dissolved O_2, free dissolved CO_2 and respiration rates in the Piracicaba River basin, southeast Brazil. Water Res. 33, 2119–2129.

Beer, T., 1983. Environmental Oceanography: An Introduction to the Behavior of Coastal Waters. Pergamon Press, Oxford. 226 pp.

Benson, B.B., Krause, J.R., 1984. The concentration and isotopic fractionation of oxygen dissolved in freshwater and seawater in equilibrium with atmosphere. Limnol. Oceanogr. 29, 620–632.

Biswas, H., Mukhopadhyay, S.K., De, T.K., Sen, S., Jana, T.K., 2004. Biogenic controls on the air–water carbon dioxide exchange in the Sundarban mangrove environment, northeast coast of Bay of Bengal, India. Limnol. Oceanogr. 49, 95–101.

Borges, A.V., 2005. Do we have enough pieces of the jigsaw to integrate CO_2 fluxes in the coastal ocean? Estuaries 28 (1), 3–27.

Borges, A.V., Delille, B., Schiettecatte, L.-S., Gazeau, F., Abril, G., Frankignoulle, M., 2004a. Gas transfer velocities of CO_2 in three European estuaries (Randers Fjord, Scheldt, and Thames). Limnol. Oceanogr. 49, 1630–1641.

Borges, A.V., Vanderborght, J.-P., Schiettecatte, L.-S., Gazeau, F., Ferrón-Smith, S., Delille, B., Frankignoulle, M., 2004b. Variability of the gas transfer velocity of CO_2 in a macrotidal estuary (the Scheldt). Estuaries 27, 593–603.

Borges, A.V., Schiettecatte, L.-S., Abril, G., Delille, B., Gazeau, F., 2006. Carbon dioxide in European coastal waters. Estuar. Coast. Shelf Sci. 70 (3), 375–387.

Brasse, S., Nellen, M., Seifert, M., Michaelis, W., 2002. The carbon dioxide system in the Elbe estuary. Biogeochemistry 59 (1), 25–40.

Cai, W.-J., 2003. Riverine inorganic carbon flux and rate of biological uptake in the Mississippi River plume. Geophys. Res. Lett. 30 (2), 1029–1032.

Cai, W.-J., Wang, Y., 1998. The chemistry, fluxes, and sources of carbon dioxide in the estuarine waters of the Satilla and Altamaha Rivers, Georgia. Limnol. Oceanogr. 43, 657–668.

Carini, S., Weston, N., Hopkinson, C., Tucker, J., Giblin, A., Vallino, J., 1996. Gas exchange rates in the Parker River estuary, Massachusetts. Biol. Bull. 191, 333–334.

Clark, F., Simpson, H.J., Smethie, W.M., Toles, C., 1992. Gas exchange in a contaminated estuary inferred from chlorofluorocarbons. Geophys. Res. Lett. 19, 1133–1136.

Clark, J.F., Schlosser, P., Simpson, H.J., Stute, M., Wanninkhof, R., Ho, D.T., 1995. Relationship between gas transfer velocities and wind speeds in the tidal Hudson River determined by the dual tracer technique. In: Jhane, B., Monahan, E. (Eds.), Air–Water Gas Transfer. AEON Verlag and Studio, Hanau, Germany, pp. 785–800.

DeGrandpre, M.D., Hammar, T.R., Wallace, D.W.R., Wirick, C.D., 1997. Simultaneous mooring-based measurements of seawater CO_2 and O_2 off Cape Hatteras, North Carolina. Limnol. Oceanogr. 42, 21–28.

Devol, A.H., Quay, P.D., Richey, J.E., Martinelli, L.A., 1987. The role of gas exchange in the inorganic carbon, oxygen, and ^{222}Rn budgets of the Amazon River. Limnol. Oceanogr. 32, 235–248.

Frankignoulle, M., Abril, G., Borges, A., Bourge, I., Canon, C., Delille, B., Liebert, E., Theate, J.-M., 1998. Carbon dioxide emission from European estuaries. Science 282, 434–436.

García-Luque, E., Forja, J.M., Gómez-Parra, A., 2005. Characterization of atmosphere–water exchange processes of CO_2 in estuaries using dynamic simulation. J. Mar. Syst. 58, 98–106.

Hellings, L., Dehairs, F., Van Damme, S., Baeyens, W., 2001. Dissolved inorganic carbon in a highly polluted estuary (the Scheldt). Limnol. Oceanogr. 46 (6), 1406–1414.

Howland, R.J.M., Tappin, A.D., Uncles, R.J., Plummer, D.H., Bloomer, N.J., 2000. Distribution and seasonal variability of pH and alkalinity in the Tweed Estuary, UK. Sci. Total Environ. 251/252, 125–138.

Huertas, E., Navarro, G., Rodríguez-Galvez, S., Lubián, L.M., 2006. Temporal patterns of carbon dioxide in relation to hydrological conditions and primary production in the northeastern shelf of the Gulf of Cadiz (SW Spain). Deep-Sea Res., Part 2, Top. Stud. Oceanogr. 53, 1344–1362.

Jahnke, R.A., Jahnke, D.B., 2000. Rates of C, N, P and Si recycling and denitrification at the US Mid-Atlantic continental slope depocenter. Deep-Sea Res., Part 1, Oceanogr. Res. Pap. 47, 1405–1428.

Khoo, K.H., Ramette, R.W., Culberson, C.H., Bates, R.G., 1977. Determination of hydrogen ion concentrations in seawater from 5 to 40 °C: standard potentials at salinities from 20 to 45‰. Anal. Chem. 49 (1), 29–34.

Körtzinger, A., Thomas, H., Schneider, B., Gronau, N., Mintrop, L., Duinker, J.C., 1996. At-sea intercomparison of two newly designed underway pCO$_2$ systems — encouraging results. Mar. Chem. 52, 133–145.

Liss, P.S., 1976. Conservative and non-conservative behaviour of dissolved constituents during estuarine mixing. In: Burton, J.D., Liss, P.S. (Eds.), Estuarine Chemistry. Academic Press, New York, pp. 93–130.

Marino, R., Howarth, R.W., 1993. Atmospheric oxygen exchange in the Hudson River: dome measurements and comparison with other natural waters. Estuaries 16, 433–445.

Mucci, A., 1983. The solubility of calcite and aragonite in seawater at various salinities, temperatures and one atmosphere total pressure. Am. J. Sci. 283, 780–799.

Neubauer, S.C., Anderson, I.C., 2003. Transport of dissolved inorganic carbon from a tidal freshwater marsh to the York River estuary. Limnol. Oceanogr. 48, 299–307.

O'Connor, D.J., Dobbins, W.E., 1958. Mechanism of re-aeration in natural streams. Trans. Am. Soc. Civ. Eng. 123, 641–684.

Perez, F.F., Fraga, F., 1987. A precise and rapid analytical procedure for alkalinity determination. Mar. Chem. 21, 169–182.

Raymond, P.A., Cole, J.J., 2001. Gas exchange in rivers and estuaries: choosing a gas transfer velocity. Estuaries 24, 312–317.

Raymond, P.A., Cole, J.J., 2003. Increase in the export of alkalinity from North America's largest river. Science 301, 88–91.

Raymond, P.A., Caraco, N.F., Cole, J.J., 1997. Carbon dioxide concentrations and atmospheric fluxes in the Hudson River. Estuaries 20, 381–390.

Roy, S., Gaillardet, J., Allègre, C.J., 1999. Geochemistry of dissolved and suspended loads of the Seine river, France: anthropogenic impact, carbonate and silicate weathering. Geochim. Cosmochim. Acta 63 (9), 1277–1292.

Sabine, C.L., Feely, R.A., Gruber, N., Key, R.M., Lee, K., Bullister, J.L., Wanninkhof, R., Wong, C.S., Wallace, D.W.R., Tilbrook, B., Millero, F.J., Peng, T.-H., Kozyr, A., Ono, T., Rios, A.F., 2004. The oceanic sink for anthropogenic CO_2. Science 305, 367–371.

Smith, S., Hollibaugh, J.T., 1993. Coastal metabolism and the oceanic carbon balance. Rev. Geophys. 31, 75–89.

Wang, Z.A., Cai, W.-J., 2004. Carbon dioxide degassing and inorganic carbon export from a marsh-dominated estuary (the Duplin River): a marsh CO_2 pump. Limnol. Oceanogr. 49, 341–354.

Wanninkhof, R., 1992. Relationship between wind speed and gas exchange over the ocean. J. Geophys. Res. 97 (C5), 7373–7382.

Weiss, R.F., 1974. Carbon dioxide in water and seawater: the solubility of a non-ideal gas. Mar. Chem. 2, 203–215.

Wollast, R., 1998. Evaluation and comparison of the global carbon cycle in the coastal zone and in the open ocean. In: Brink, K.H., Robinson, A.R. (Eds.), The Global Coastal Ocean, vol. 10. John Wiley & Sons, New York, pp. 213–252.

Zappa, C.J., Raymond, P.A., Terray, E.A., McGillis, W.R., 2003. Variation in surface turbulence and the gas transfer velocity over a tidal cycle in a macro-tidal estuary. Estuaries 26, 1401–1415.

Zhai, W.Z., Dai, M., Cai, W.-J., Wang, Y., Wang, Z., 2005. High partial pressure of CO_2 and its maintaining mechanism in a subtropical estuary: the Pearl River estuary, China. Mar. Chem. 93, 21–32.